Prediction of high-T_c conventional superconductivity in the ternary lithium borohydride system

Christian Kokail,[1,*] Wolfgang von der Linden,[1] and Lilia Boeri[1,2]
[1]*Institute of Theoretical and Computational Physics, Graz University of Technology, NAWI Graz, 8010 Graz, Austria*
[2]*Dipartimento di Fisica, Sapienza Università di Roma, 00185 Roma, Italy*
(Received 20 May 2017; revised manuscript received 27 August 2017; published 11 December 2017)

We investigate the superconducting ternary lithium borohydride phase diagram at pressures of 0 and 200 GPa using methods for evolutionary crystal structure prediction and linear-response calculations for the electron-phonon coupling. Our calculations show that the ground state phase at ambient pressure, $LiBH_4$, stays in the *Pnma* space group and remains a wide band-gap insulator at all pressures investigated. Other phases along the 1:1:x Li:B:H line are also insulating. However, a full search of the ternary phase diagram at 200 GPa revealed a metallic Li_2BH_6 phase, which is thermodynamically stable down to 100 GPa. This *superhydride* phase, crystallizing in a $Fm\bar{3}m$ space group, is characterized by sixfold hydrogen-coordinated boron atoms occupying the fcc sites of the unit cell. Due to strong hydrogen-boron bonding this phase displays a critical temperature of ∼100 K between 100 and 200 GPa. Our investigations confirm that ternary compounds used in hydrogen-storage applications should exhibit high-T_c conventional superconductivity in diamond anvil cell experiments, and suggest a viable route to optimize the superconducting behavior of high-pressure hydrides, exploiting metallic covalent bonds.

DOI: 10.1103/PhysRevMaterials.1.074803

The pioneering prediction of Ashcroft that hydrogen, the lightest among all elements, could become a high-temperature (high-T_c) superconductor at high pressures, can be seen as the foundation of high-pressure superconductivity research [1]. Besides pure hydrogen, Ashcroft postulated that also metallic hydrides can become high-T_c superconductors at much lower pressures than those required to metallize hydrogen [2], since impurities in the hydrogen matrix can influence the bonding properties, and cause a *chemical precompression* on the H atoms [3,4]. This idea has led to the prediction of novel high-pressure hydrides, with remarkable superconducting transition temperatures [3,5–11]. The coronation of this prediction was the experimental discovery of superconductivity with a critical temperature (T_c) of 203 K in a sulfur hydride (SH_3) at 200 GPa [12–14]. In addition to setting a new record of T_c, this compound was an example of an unknown superconductor entirely predicted from first principles. A few months after SH_3, high-T_c superconductivity was reported in a second superconducting hydride PH_3 [15–18].

Several *ab initio* studies have permitted us to understand that the record-high T_c of SH_3 is a consequence of high electron-phonon (*ep*) matrix elements enabled by the strong hydrogen-sulfur bonds, electronic van Hove singularities at the Fermi level, and large vibrational frequencies of the hydrogen modes accompanied by strong anharmonic effects [14,19–26]. The first two aspects are intrinsically related to the $Im\bar{3}m$ high-pressure structure of SH_3, in which sulfur forms three 90° covalent bonds with hydrogen.

The formation of metallic covalent bonds is an essential ingredient for high-T_c conventional superconductivity, because this kind of bond experiences the strongest coupling to phonons. Phases with metallic covalent bonds are extremely rare at ambient pressures—MgB_2, B-doped diamond, and graphane are a few examples; At high pressures they can be stabilized in binary hydrides that contain elements with electronegativities close to that of hydrogen [17,19,20]. Electronegativity is thus one of the main external parameters affecting the high-pressure superconducting behavior of hydrides, but it is likely that also other atomic properties, such as valence, atomic radii, etc., play a similar role. Understanding how these properties could be tuned to increase the maximum critical temperatures or decrease the pressure needed to induce high-T_c superconductivity represents a major step forward for the design of better superconductors.

A viable strategy is suggested by hydrogen storage research. In fact, *complex* (ternary or higher) hydrides often exhibit improved performances compared to simple hydrides, because by combining weak and strong hydride formers it is possible to affect independently different properties, such as hydrogen density and activation barriers [27]. Similarly, at high pressures one could exploit the chemical flexibility of complex hydrides to tune independently the doping level and the bonding characteristics to lower the metallization pressure or increase the maximum T_c compared to binary hydrides.

In this work we explore this route computing *ab initio* the high-pressure superconducting phase diagram of a prototypical ternary system, lithium-boron-hydrogen, combining methods for evolutionary crystal structure prediction with linear-response calculations of the electron-phonon (*ep*) coupling [28,29]. Our aim is to identify prospective high-T_c superconductors at high pressures. We show that an accurate sampling of the whole phase diagram is needed to identify the high-T_c superconducting phases, because these are found for compositions that are not *obvious* in the sense that will be discussed below.

The lithium-boron-hydrogen system is very well characterized at ambient pressures, because ground-state lithium borohydride ($LiBH_4$) is one of the best materials for hydrogen storage applications. This compound combines a weak (Li) and a strong (B) hydride former, and this permits us to have at the same time a high hydrogen density and a reasonable activation barrier for hydrogenation and dehydrogenation reactions; due to the low masses of Li and B, not only the volumetric density,

*ckokail@alumni.tugraz.at

 ©2017 American Physical Society

but also the gravimetric one, are extremely high [30–37]. Furthermore, the existence of several possible hydriding and dehydriding reactions provides the possibility to control the H content in experiments [38,39].

Except for the boundary phases (Li-B, Li-H, B-H), the high-pressure phase diagram is unknown, but there are many reasons to believe that it could host high-T_c superconductors. First of all, the very light masses of the three constituents imply that the average phonon frequencies of all compounds will be high, which is intrinsically favorable to phonon-mediated superactivity. In fact Li, B, and the corresponding hydrides exhibit interesting superconducting properties under pressure [5,40–49], while the binary Li-B system hosts one of the first *ab initio* predictions of novel superconductors [50]. Furthermore, strong hydride formers, such as boron, form covalent or ionic bonds, which translate into large intrinsic *ep* matrix elements, while weak hydride formers typically form metallic hydrides; combining the properties of the two elements, therefore, a ternary Li-B-H compound could behave as a "covalent metal," similarly to SH_3, already at much lower pressures. The many hydrogen-rich phases which are weakly metastable at ambient pressure are ideal candidates for covalent metallic behavior (and superconductivity): in fact, they could be considered the ternary equivalent of SH_3, which is a hydrogen-rich phase obtained by the hydring reaction of SH_2 at high pressures [12,14].

The aim of this work is to understand whether any of the ternary Li-B-H compounds known at ambient pressure, or any new, still unknown composition, exhibit high-T_c superconductivity in the Megabar range. We indeed identify a new high-T_c phase (Li_2BH_6), which, similarly to SH_3, can be classified as a highly symmetric covalent metal. At 200 GPa, this compound exhibits a T_c of 80 K, i.e., lower than SH_3 but, in contrast to other known hydrides, the high-T_c behavior persists down to 100 GPa. We will argue that the possibility to lower the pressure for high-T_c compared to binary hydrides is an intrinsic property of ternary (or higher) hydrides.

Figure 1 shows the phase diagram of the Li-B-H system at ambient pressure ($P = 0$) and at 200 GPa ($P = 200$), calculated using the evolutionary crystal structure prediction method, as implemented in the USPEX code [51–54]. Due to the high computational cost of ternary phase diagrams, we had to restrict our search to representative pressures: 200 GPa was chosen because this is the pressure at which SH_3 exhibits its maximum T_c, and is well beyond the metallization pressure for many binary hydrides. Ambient pressure was mainly intended to check the accuracy of our calculations against literature results.

We first performed a full search of the two ternary phase diagrams, in which we sampled many possible compositions, represented by symbols in the two upper panels. The aim of this preliminary scan is to identify the compositions in the ternary phase diagram that could give rise to high-symmetry metallic structures at high pressure. In order to ensure an optimal trade-off between accuracy and computational time, we restricted the search to structures with all possible compositions, but with a minimum (maximum) number of atoms/unit cell equal to 8 (16); a combinatorial argument gives a total of 300 possible stoichiometries. For each pressure, we generated a total of 1800 structures, which gives an average of 6 structures/composition. We would like to remind

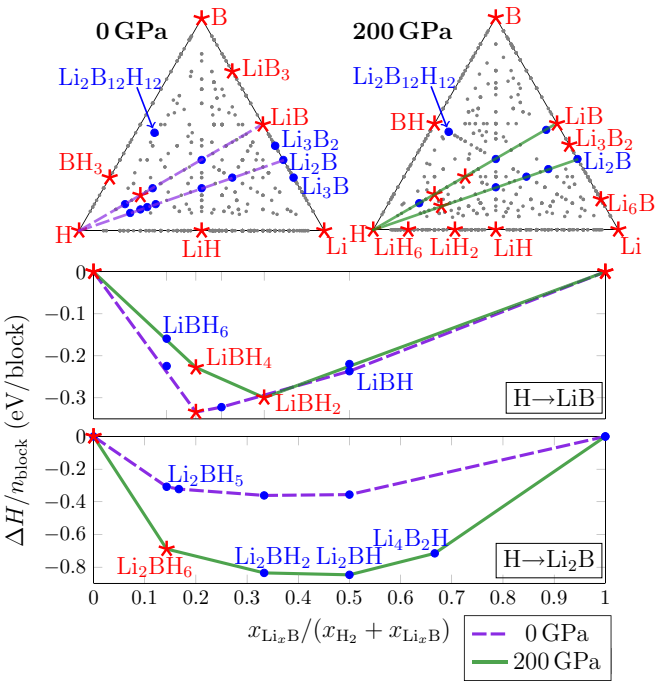

FIG. 1. *Top:* Generalized convex hull for the Li-B-H system at 0 (left) and 200 (right) GPa, obtained from evolutionary crystal structure prediction. Points represent compositions sampled in our preliminary run, lines indicate ranges of compositions for which we computed more accurate binary convex hulls (see text). These are shown in the *bottom panels*. Circles and stars represent compositions that are thermodynamically metastable or stable with respect to other phases on the ternary hull (see text).

the reader that this is only an exploratory run, while more accurate runs were used to inspect the most promising compositions [55].

Despite the apparently coarse sampling, our preliminary search identified correctly all known Li-B-H phases, both along the boundary lines and in the middle of the phase diagram. Several ambient pressure hydrogen-rich phases reported in literature, with chemical formula $Li(BH)_x$ [34,56,57], are correctly reproduced by our search, but not discussed in the following, because they do not lie on the ambient-pressure convex hull and are not relevant to our discussion of phases stabilized in the Megabar range. $Li_2B_{12}H_{12}$, which is an important intermediate product of the hydrogenation process of $LiBH_4$ [34], has been added by hand, because the unit cell at ambient pressure is larger than the maximum number of atoms employed for our search. At ambient pressure, we reproduce the phase diagram and energetics of previous works; at $P = 200$ GPa, there are no literature data for ternary phases, but we reproduce known results for the Li-H, B-H, and Li-B systems [5,49,50].

Our previous experience on binary systems taught us that the energies and structures from initial coarse sampling runs need to further be refined to obtain a correct ranking of structures and compositions [46]. For this reason, after the initial scan, we focused onto two specific Li:B:H lines, shown in Fig. 1 [58]. These are the 1:1:x line that contains compounds with chemical formula $LiBH_x$, including $LiBH_4$, and the 2:1:x

one, where we found a highly symmetric metallic structure with chemical formula Li_2BH_6. For these two lines, we ran additional crystal structure prediction runs with tighter settings; the same was done for boundary lines, and for $Li_2B_{12}H_{12}$.

The two enthalpy (ΔH) vs composition (x) binary convex hulls are shown in the two lower panels of Fig. 1.

Similarly to what observed in binary hydrides, pressures in the Megabar range stabilize several compositions which are metastable at ambient pressure. In particular, along the 1:1:x line LiBH, $LiBH_2$, and $LiBH_6$, besides the ground-state $LiBH_4$, lie close to the hull, while for the 2:1:x line there are several compositions close to the hull. Note that compositions on the binary hull are stable with respect to the decomposition into the end members of the line (LiB + H and Li_2B + H); however, in a ternary system other decompositions are also possible. Although computing all possible paths would be prohibitive, we recomputed the enthalpy of formation of all compounds on the binary hulls also with respect to boundary phases; taking this effect into account, a few phases on the binary hull turned out to be metastable. These are shown as (blue) circles in Fig. 1, while genuinely ground state structures are shown as (red) stars. In the following, we will discuss the crystal and electronic structure of the most interesting compositions, with the aim of identifying potential high-T_c superconductors. The details of the relative crystal structures can be found in the Supplemental Material [59].

We start from the ground-state $LiBH_4$, shown in the upper panel of Fig. 2. For this stoichiometry, we ran evolutionary structure prediction runs at fixed compositions for 0, 100, 200, and 300 GPa with 2, 3, and 4 formula units per unit cell. At all pressures, we found as most stable a *Pmma* structure, in which $(BH_4)^-$ tetrahedra are intercalated with Li^+ ions. At ambient pressure, the structure is very open, and the BH_4 tetrahedra can orient freely in the unit cell. Pressure leads to a more close-packed arrangement, in which the BH_4 tetrahedra only acquire two possible orientations around the Li atoms. The high-pressure structure shown in the figure is stable at least up to 300 GPa, where it is still insulating. Thus, $LiBH_4$ cannot support high-T_c conventional superconductivity as in SH_3, but other phases on the phase diagrams are strong candidates.

An obvious candidate, due to its high hydrogen content, is $Li_2B_{12}H_{12}$. At ambient pressure, this compound crystallizes in an open structure of B-H icosahedra, intercalated with lithium atoms. Icosahedra are found in α-boron and in several B-rich phases, including superconducting dodecaborides, such as ZrB_{12} [60]. However, at ambient pressure $Li_2B_{12}H_{12}$ is insulating, and hence cannot superconduct. At higher pressures, the eicosahedral environment is destabilized, and $Li_2B_{12}H_{12}$ acquires a completely different structure, characterized by unidimensional B-H chains [49], intercalated by lithium. This phase is however metastable (by 200 meV/atom) with respect to elemental decomposition, and we will not consider it further in our study.

Other compounds which have been often discussed in the hydrogenation and rehydrogenation reactions of $LiBH_4$ are those that lie along the 1:1:x Li:B:H line. The bottom left panel of Fig. 2 shows the high-pressure crystal structure of $LiBH_6$. The high-pressure stabilization of a hydrogen-rich phase of $LiBH_4$ could be the analog of the reaction

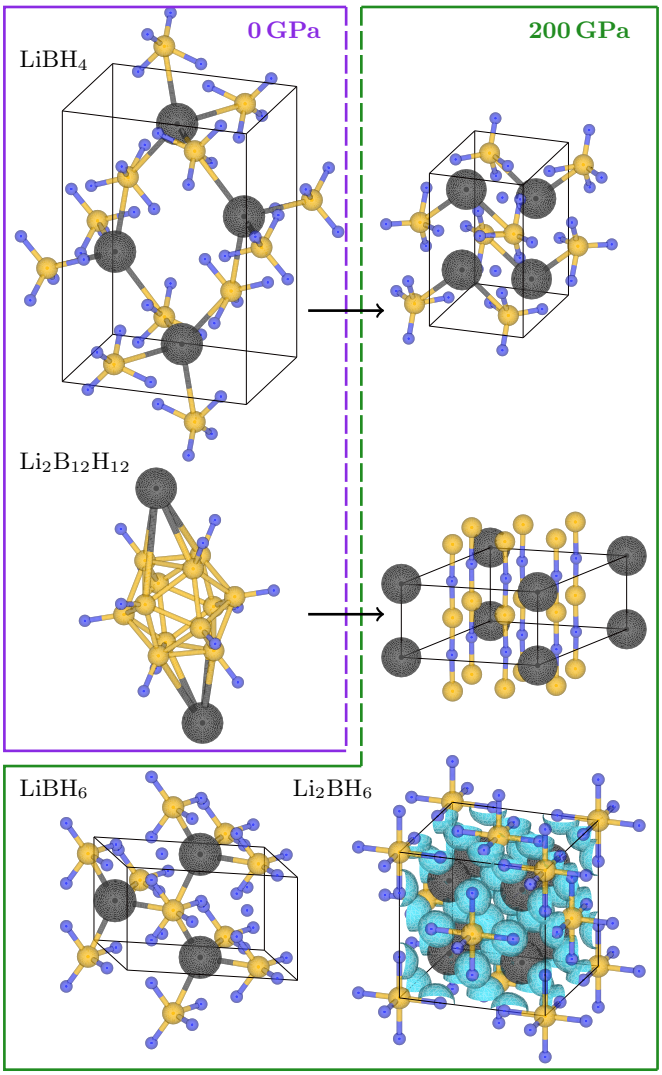

FIG. 2. Crystal structure of selected Li-B-H phases at 0 and 200 GPa identified in this work. For Li_2BH_6, we also plot the 0.7 ELF isocontour.

$SH_2 + H_2 \rightarrow SH_3$ that led to the discovery of the first high-pressure conventional superconductor. However, Fig. 2 shows that there is an important difference between SH_3 and $LiBH_6$. In SH_3 a pressure of 200 GPa is sufficient to break the molecular bonds of SH_2 and H_2 and stabilize three new directional, covalent bonds between S and H. In $LiBH_6$ one can still recognize a close-packed $LiBH_4$ lattice, and molecular hydrogen intercalated in-between. This structure should thus rather be described as $LiBH_4 + H_2$ than $LiBH_6$. Not surprisingly, this structure is insulating.

Our evolutionary runs allowed us to identify at least one hydrogen-rich phase in which the (BH_4) tetrahedral environment is destabilized, and molecular hydrogen is incorporated into the boron lattice. This is the Li_2BH_6 structure shown in the bottom right panel of Fig. 2. Here boron and hydrogen form octahedra, and lithium sits in-between. BH_6 octahedra are not common in nature, but an AlH_6 octahedral motif is common in alanates [61,62]. For borohydrides this motif, which is stabilized by e_g (d) electrons, has never been observed

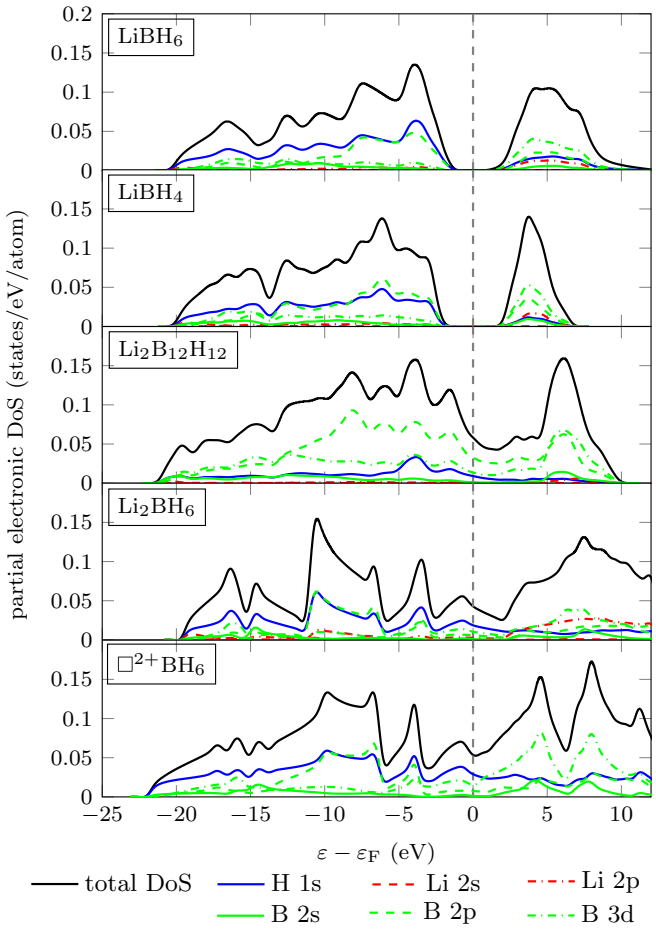

FIG. 3. Partial density of states (pDOS) of the most representative phases analysed in this work. All DOS have been calculated at 200 GPa. From top to bottom: $LiBH_6$, $LiBH_4$, $Li_2B_{12}H_{12}$, Li_2BH_6, and a hypothetical compound in which Li has been replaced by a uniform, positive background of charge ($\square^{+2}BH_6$).

at ambient pressure, and we consider our finding an example of high-pressure forbidden chemistry; we will come back to this point in the following.

Although unusual in structure and composition, according to our calculations Li_2BH_6 remains thermodynamically stable with respect to decompositions towards all phases on the ternary Gibbs diagram down to 100 GPa. Given the accuracy of our predictions in all other cases for which we had access to experimental data, we believe that this is a strong indication that Li_2BH_6 could be synthesized in experiments. In Fig. 2, superimposed to the crystal structure of Li_2BH_6, we show the 0.7 isocontour of the electronic localization function (ELF); the plot shows that most of the charge resides along the BH_6 bonds. Combined with the fact that Li_2BH_6 is metallic, this makes it a very strong candidate for high-T_c conventional superconductivity. Indeed, as we will show, our electronic structure calculations confirm this hypothesis.

Figure 3 shows the partial densities of states (DOS) of the most relevant ternary Li:B:H phases in this work, calculated at 200 GPa. The first two panels show $LiBH_4$ and $LiBH_6$; in both compounds a large gap ($\Delta \sim 3$ eV) separates bonding and antibonding states derived from the hybridization of B sp^3 states with hydrogen. This makes the BH_4 environment extremely stable; in fact, in $LiBH_6$ the two excess hydrogens do not bind to boron, but remain in molecular form, and arrange in the interstitials of the structure; the relative electronic states form an additional peak near the top of the valence band. Other structures along the 1:1:x line (not shown) are also insulating for similar reasons at this pressure. $Li_2B_2H_{12}$, shown immediately below, is a good metal, but metastable.

The two bottom panels show $Li_2B_6H_6$, which is the most promising candidate for superconductivity identified in this work, and a hypothetical compound in which lithium is replaced by a uniform background of charge ($\square^{+2}BH_6$). The strong similarity between the two DOS in the valence region indicates that the main role of lithium in this structure is to donate charge to the boron-hydrogen octahedra, while its contribution to the bonding is only marginal.

We can thus try to understand the electronic structure in terms of the BH_6 cluster alone; the states at the Fermi level result from the hybridization of B d e_g states with hydrogen; the two other structures centered at ~ -8 and ~ -15 eV correspond to B s and p states. It has been argued that the octahedral environment is not seen in borohydrides, because the gap between d and p states is too large compared to other hydrides of the third group. In these compounds, the XH_6 environment is stable already at ambient pressure, where the bandwidth is much smaller. s, p, and e_g states cause clear gaps in the electronic spectrum. Octahedral hydrides typically host 12 valence electrons, corresponding to a complete filling of s, p, and e_g shells. On the other hand, according to our calculations, the Li_2BH_6 phase, which has only 11 valence electrons, is thermodynamically stable down to 100 GPa, where it remains metallic. We believe that the reason why this unusual phase can occur at high pressures is that the boron-hydrogen bandwidth is large enough to overcome the intrinsic gaps in the boron spectrum, giving rise to a metallic DOS, allowing a wider range of dopings. In Li2BH_6, the Fermi level sits in a shallow region of this continuum, where $N \sim 0.2$ st/eV f.u.

In order to estimate the actual superconducting characteristics of Li_2BH_6, we performed linear response calculations [28] of its electron-phonon properties, and estimated the critical temperature through the McMillan-Allen-Dynes formula [63,64]:

$$T_c = \frac{\omega_{\log}}{1.2k_B} \exp\left[-\frac{1.04(1+\lambda)}{\lambda - \mu^\star(1+0.62\lambda)}\right]. \quad (1)$$

The phonon dispersions, decorated with circles whose size is proportional to the partial ep coupling of each branch, are shown in the left panels of Fig. 4; the right panels shows the partial phonon DOS and the ep (Eliashberg) spectral function $\alpha^2F(\omega)$, which describes how the ep coupling is distributed on phonon modes with energy ω. The top and bottom panels refer to $P = 100$ and $P = 200$ GPa, respectively. The parameters λ (ep coupling constant) and $\omega_{\log}$ (logaritmically averaged phonon frequency) in Eq. (1) can be obtained from $\alpha^2F(\omega)$ as $\lambda = 2\int d\omega \frac{\alpha^2F(\omega)}{\omega}$ and $\omega_{\log} = \exp\left[\frac{2}{\lambda}\int \frac{d\omega}{\omega}\alpha^2F(\omega)\ln(\omega)\right]$; $\mu^\star$ is the Coulomb pseudopotential, renormalized to include retardation effects due to the large disparity between the electron and phonon energies.

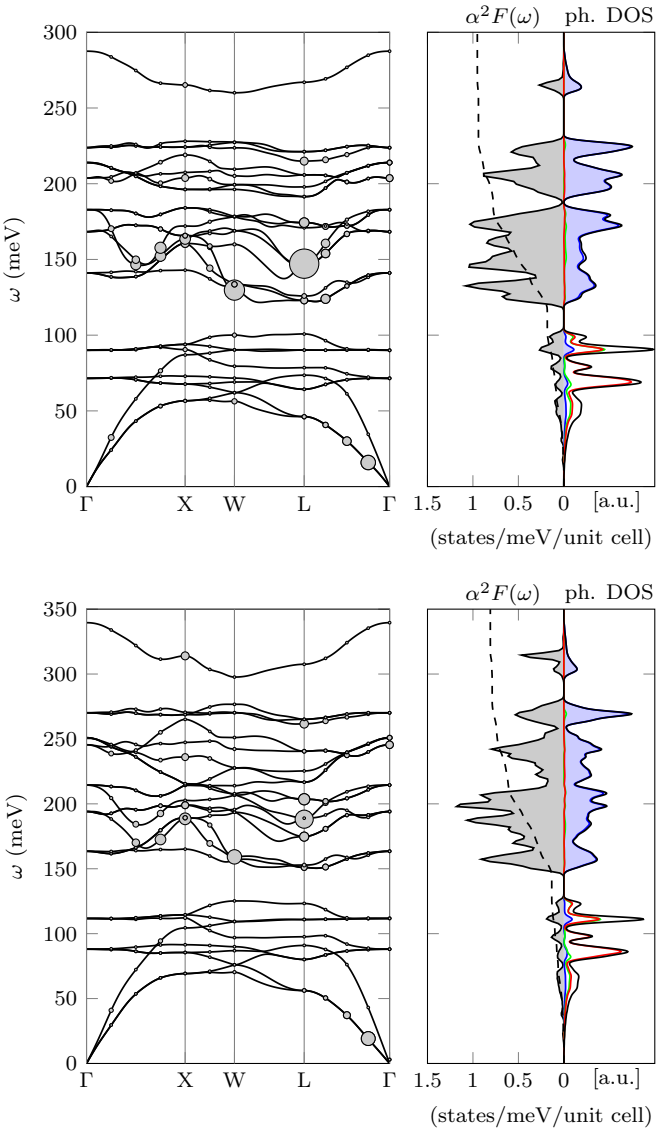

FIG. 4. Phonon dispersions (left), densities of states, and *ep* spectral function (right) of Li_2BH_6 at 100 (top) and 200 (bottom) GPa. The size of the circles in the phonon dispersion plot is proportional to the partial *ep* coupling constant for a given mode. The colors in the DOS plot indicate partial contributions; the color coding is the same as in Fig. 3.

For $P = 100$ and 200 GPa, we obtain $\omega_{\log} = 1551$ and 1940 K and $\lambda = 0.94$ and 0.76, respectively. The corresponding T_c, estimated from Eq. (1) with $\mu^* = 0.1$ are 98 and 81 K, comparable to those of PH_3. Comparing the $\alpha^2F(\omega)$ with the partial phonon DOS next to it, it is clear that the most substantial contribution to the coupling comes from H modes at intermediate frequencies, while octahedral vibrations (above 300 meV) play a very marginal role. The phonon spectrum shifts almost rigidly by ∼50 meV going from 100 to 200 GPa, causing a similar increase in $\omega_{\log}$. On the other hand, the DOS at the Fermi level decreases by 20%, causing a similar decrease in the total *ep* coupling constant. The factor $\tilde{\eta} = \lambda/N(E_F)$, which is a measure of the lattice contribution to the *ep* coupling, is almost constant $\tilde{\eta} \simeq 4.2$ eV f.u., and comparable with SH_3 and PH_3, where $\tilde{\eta}$ is 3.6 and 3.8, respectively [18]. Figure 3 shows that the Fermi level in Li_2BH_6 sits in a shallow region of the DOS, which is weakly affected by pressure; this explains the weak dependence of T_c on P.

While this weak dependence implies that T_c cannot be effectively boosted by pressure, as in PH_3 and SH_3, it also implies that superconductivity survives with remarkable T_c down to pressures which are twice as small than in SH_3. Furthermore, the fact that the atoms that contribute to charge doping and covalent bonding are different (lithium and boron, respectively), offers a simple route to improve the superconducting properties of Li_2BH_6. Partially replacing lithium with alkaline earths or vacancies would allow us to easily tune the doping level, and hence the value of the DOS, without affecting the stiff boron-hydrogen sublattice responsible for the large *ep* coupling. Doping on the Li site in ternary hydrides is routinely achieved in hydrogen storage applications, and is most likely much easier to obtain also at high pressures than the iso- or heterovalent substitutions proposed by several authors for covalent hydrides [10,20,65]. Based on a simple rigid-band argument, we estimate that introducing 10%–15% Li-vacancies could increase the T_c at 200 GPa by more than 50%, up to 133 K. On the other hand, substitutions at the B site could be used to tune other intrinsic properties, such as *ep* matrix elements or metallization pressures.

In conclusion, in this work we have studied from first principles the high-pressure superconducting phase diagram of lithium-boron-hydrogen, a prototypical ternary system employed for hydrogen storage applications. Besides the well-known boundary phases, we have identified several new compositions which are stabilized by high pressures. We have shown that neither the ground-state $LiBH_4$, nor any of its direct hydrogenation or dehydrogenation products, is a viable candidate for high-T_c superconductivity, but we have identified at least one ternary phase Li_2BH_6, which exhibits superconducting properties comparable to those of the best binary hydrides. The Li_2BH_6 composition is not stable at ambient pressure, but according to our calculations it should become thermodynamically stable for $P > 100$ GPa. Similarly to SH_3, which is a hydrogen-rich phase of sulfur hydride, in which the original molecular bonds are broken and new, directional bonds are formed under pressure, Li_2BH_6 exhibits a highly symmetric structure in which the original BH_4 tetrahedra that are characteristic of boronhydrides rearrange to form BH_6 octahedra, with covalent B-H bonds. These determine the valence band structure, while lithium mainly acts as a charge reservoir. The fact that two different atoms govern the bonding and the charge doping should allow us to tune the T_c more easily than in binary hydrides. Our work demonstrates that ternary hydrides can exhibit high-T_c superconductivity and is a first step towards the optimization of superconducting properties in high-pressure hydrides using chemical methods.

The authors acknowledge computational resources from the dCluster of the Graz University of Technology and the VSC3 of the Vienna University of Technolog, and support through the FWF, Austrian Science Fund, Project P 30269-N36 (*Superhydra*).

[1] N. W. Ashcroft, Phys. Rev. Lett. **21**, 1748 (1968).
[2] N. W. Ashcroft, Phys. Rev. Lett. **92**, 187002 (2004).
[3] Y. Yao and D. D. Klug, Proc. Natl. Acad. Sci. USA **107**, 20893 (2010).
[4] J. Feng, W. Grochala, T. Jaroń, R. Hoffmann, A. Bergara, and N. W. Ashcroft, Phys. Rev. Lett. **96**, 017006 (2006).
[5] E. Zurek, R. Hoffmann, N. Ashcroft, A. R. Oganov, and A. O. Lyakhov, Proc. Natl. Acad. Sci. USA **106**, 17640 (2009).
[6] D. Y. Kim, R. H. Scheicher, H.-k. Mao, T. W. Kang, and R. Ahuja, Proc. Natl. Acad. Sci. USA **107**, 2793 (2010).
[7] H. Wang, J. S. Tse, K. Tanaka, T. Iitaka, and Y. Ma, Proc. Natl. Acad. Sci. USA **109**, 6463 (2012).
[8] Y. Li, J. Hao, H. Liu, J. S. Tse, Y. Wang, and Y. Ma, Sci. Rep. **5**, 9948 EP (2015).
[9] V. V. Struzhkin, Physica C **514**, 77 (2015).
[10] J. A. Flores-Livas, A. Sanna, M. Grauzinyte, A. Davydov, S. Goedecker, and M. A. L. Marques, Sci. Rep. **7**, 6825 (2017).
[11] A. Shamp and E. Zurek, J. Phys. Chem. Lett. **6**, 4067 (2015).
[12] A. P. Drozdov, M. I. Eremets, I. A. Troyan, V. Ksenofontov, and S. I. Shylin, Nature (London) **525**, 73 (2015).
[13] I. Troyan, A. Gavriliuk, R. Rüffer, A. Chumakov, A. Mironovich, I. Lyubutin, D. Perekalin, A. P. Drozdov, and M. I. Eremets, Science **351**, 1303 (2016).
[14] D. Duan, Y. Liu, F. Tian, D. Li, X. Huang, Z. Zhao, H. Yu, B. Liu, W. Tian, and T. Cui, Sci. Rep. **4**, 6968 (2014).
[15] A. P. Drozdov, M. I. Eremets, and I. A. Troyan, arXiv:1508.06224.
[16] A. Shamp, T. Terpstra, T. Bi, Z. Falls, P. Avery, and E. Zurek, J. Am. Chem. Soc. **138**, 1884 (2016).
[17] Y. Fu, X. Du, L. Zhang, F. Peng, M. Zhang, C. J. Pickard, R. J. Needs, D. J. Singh, W. Zheng, and Y. Ma, Chem. Mater. **28**, 1746 (2016).
[18] J. A. Flores-Livas, M. Amsler, C. Heil, A. Sanna, L. Boeri, G. Profeta, C. Wolverton, S. Goedecker, and E. K. U. Gross, Phys. Rev. B **93**, 020508 (2016).
[19] N. Bernstein, C. S. Hellberg, M. D. Johannes, I. I. Mazin, and M. J. Mehl, Phys. Rev. B **91**, 060511 (2015).
[20] C. Heil and L. Boeri, Phys. Rev. B **92**, 060508 (2015).
[21] J. A. Flores-Livas, A. Sanna, and E. K. Gross, Eur. Phys. J. B **89**, 63 (2016).
[22] Y. Quan and W. E. Pickett, Phys. Rev. B **93**, 104526 (2016).
[23] Y. Li, J. Hao, H. Liu, Y. Li, and Y. Ma, J. Chem. Phys. **140**, 174712 (2014).
[24] D. A. Papaconstantopoulos, B. M. Klein, M. J. Mehl, and W. E. Pickett, Phys. Rev. B **91**, 184511 (2015).
[25] L. Ortenzi, E. Cappelluti, and L. Pietronero, Phys. Rev. B **94**, 064507 (2016).
[26] I. Errea, M. Calandra, C. J. Pickard, J. Nelson, R. J. Needs, Y. Li, H. Liu, Y. Zhang, Y. Ma, and F. Mauri, Phys. Rev. Lett. **114**, 157004 (2015).
[27] S. Louis and Z. Andreas, Nature (London) **414**, 353 (2001).
[28] S. Baroni, S. de Gironcoli, A. Dal Corso, and P. Giannozzi, Rev. Mod. Phys. **73**, 515 (2001).
[29] P. Giannozzi, S. Baroni, N. Bonini, M. Calandra, R. Car, C. Cavazzoni, D. Ceresoli, G. L. Chiarotti, M. Cococcioni, I. Dabo, A. D. Corso, S. de Gironcoli, S. Fabris, G. Fratesi, R. Gebauer, U. Gerstmann, C. Gougoussis, A. Kokalj, M. Lazzeri, L. Martin-Samos, N. Marzari, F. Mauri, R. Mazzarello, S. Paolini, A. Pasquarello, L. Paulatto, C. Sbraccia, S. Scandolo, G. Sclauzero, A. P. Seitsonen, A. Smogunov, P. Umari, and R. M. Wentzcovitch, J. Phys.: Condens. Matter **21**, 395502 (2009).
[30] A. Züttel, P. Wenger, S. Rentsch, P. Sudan, P. Mauron, and C. Emmenegger, J. Power Sources **118**, 1 (2003).
[31] J. J. Vajo, S. L. Skeith, and F. Mertens, J. Phys. Chem. B **109**, 3719 (2005).
[32] A. Züttel, S. Rentsch, P. Fischer, P. Wenger, P. Sudan, P. Mauron, and C. Emmenegger, J. Alloys Compd. **356-357**, 515 (2003).
[33] K. Miwa, N. Ohba, S.-i. Towata, Y. Nakamori, and S.-i. Orimo, Phys. Rev. B **69**, 245120 (2004).
[34] S.-I. Orimo and Y. Nakamori, Appl. Phys. Lett. **89**, 021920 (2006).
[35] J.-P. Soulié, G. Renaudin, R. Cerný, and K. Yvon, J. Alloys Compd. **346**, 200 (2002).
[36] A. F. Gross, J. J. Vajo, S. L. Van Atta, and G. L. Olson, J. Phys. Chem. C **112**, 5651 (2008).
[37] P. Mauron, F. B. Florian, O. Friedrichs, A. Remhof, M. Bielmann, C. N. Zwicky, and A. Züttel, J. Phys. Chem. B **112**, 906 (2008).
[38] S. Orimo, Y. Nakamori, G. Kitahara, K. Miwa, N. Ohba, S. Towata, and A. Züttel, J. Alloys Compd. **404-406**, 427 (2005).
[39] A. N. Kolmogorov, S. Hajinazar, C. Angyal, V. L. Kuznetsov, and A. P. Jephcoat, Phys. Rev. B **92**, 144110 (2015).
[40] T. Juha, J.-N. Kirsi, U. Johanna, P. Elias, S. Anssi, and S. Alexander, Nature (London) **447**, 187 (2007).
[41] S. Katsuya, I. Hiroto, T. Daigoroh, Y. Takehiko, and A. Kiichi, Nature (London) **419**, 597 (2002).
[42] V. V. Struzhkin, M. I. Eremets, W. Gan, H.-k. Mao, and R. J. Hemley, Science **298**, 1213 (2002).
[43] J. Lv, Y. Wang, L. Zhu, and Y. Ma, Phys. Rev. Lett. **106**, 015503 (2011).
[44] M. Marqués, M. I. McMahon, E. Gregoryanz, M. Hanfland, C. L. Guillaume, C. J. Pickard, G. J. Ackland, and R. J. Nelmes, Phys. Rev. Lett. **106**, 095502 (2011).
[45] I. I. Naumov, R. J. Hemley, R. Hoffmann, and N. W. Ashcroft, J. Chem. Phys. **143**, 064702 (2015).
[46] C. Kokail, C. Heil, and L. Boeri, Phys. Rev. B **94**, 060502 (2016).
[47] M. I. Eremets, V. V. Struzhkin, H.-k. Mao, and R. J. Hemley, Science **293**, 272 (2001).
[48] D. A. Papaconstantopoulos and M. J. Mehl, Phys. Rev. B **65**, 172510 (2002).
[49] C.-H. Hu, A. R. Oganov, Q. Zhu, G.-R. Qian, G. Frapper, A. O. Lyakhov, and H.-Y. Zhou, Phys. Rev. Lett. **110**, 165504 (2013).
[50] A. N. Kolmogorov and S. Curtarolo, Phys. Rev. B **73**, 180501 (2006).
[51] USPEX employs an advanced evolutionary algorithm technique to find the global minimum of the energy (or enthalpy) landscape of a given system; each point of this hyperspace is generated by an *ab initio* calculation. An initial population of structures, generated randomly or according to user-specified criteria, is evolved using mechanisms from biological evolution (selection, mutation, reproduction, survival of the fitness) to minimize a *fitness* function, which is typically the internal energy (or enthalpy) of the system.
[52] A. R. Oganov and C. W. Glass, J. Chem. Phys. **124**, 244704 (2006).
[53] A. O. Lyakhov, A. R. Oganov, H. T. Stokes, and Q. Zhu, Comput. Phys. Commun. **184**, 1172 (2013).
[54] A. R. Oganov, A. O. Lyakhov, and M. Valle, Acc. Chem. Res. **44**, 227 (2011).

[55] For effectively sampling the energy landscape, we employed the antiseeds technique for all runs [53]. The underlying structural relaxations were performed using the VASP code within the all electron projector augmented wave method [66–69]. We used the Perdew-Burke-Ernzerhof parametrization for exchange-correlation potential [70]. For the evolutionary runs we used a maximal kinetic energy cutoff of 800 eV and a $\boldsymbol{k}$-point resolution of $0.04\,2\pi/$Å.

[56] A. N. Kolmogorov, R. Drautz, and D. G. Pettifor, Phys. Rev. B **76**, 184102 (2007).

[57] H. Wu, W. Tang, V. Stavila, W.Zhou, J. Rush, and T. Udovic, J. Phys. Chem. C **119**, 6481 (2015).

[58] For the most stable structures along the binary lines, we carried out restricted structural relaxations with plane wave cutoffs between 1000 and 1200 eV, with a $\boldsymbol{k}$-point resolution of $0.01\,2\pi/$Å, which ensured converge of the total energy better than 1 meV per atom. Moreover, we ensured that all stress tensors are diagonal and isotropic with fluctuations in the diagonal elements smaller than 0.1 kbar. All ionic forces are converged to values better than 1 meV/Å.

[59] See Supplemental Material at http://link.aps.org/supplemental/10.1103/PhysRevMaterials.1.074803 contains details on the crystal structures of the main new high-pressure phases identified in this work.

[60] B. T. Matthias, T. H. Geballe, K. Andres, E. Corenzwit, G. W. Hull, and J. P. Maita, Science **159**, 530 (1968).

[61] A. Peles, J. A. Alford, Z. Ma, L. Yang, and M. Y. Chou, Phys. Rev. B **70**, 165105 (2004).

[62] T. D. Huan, M. Amsler, M. A. L. Marques, S. Botti, A. Willand, and S. Goedecker, Phys. Rev. Lett. **110**, 135502 (2013).

[63] W. L. McMillan, Phys. Rev. **167**, 331 (1968).

[64] P. B. Allen and R. C. Dynes, Phys. Rev. B **12**, 905 (1975).

[65] Y. Ge, F. Zhang, and Y. Yao, Phys. Rev. B **93**, 224513 (2016).

[66] G. Kresse and J. Hafner, Phys. Rev. B **47**, 558 (1993).

[67] G. Kresse and J. Furthmüller, Phys. Rev. B **54**, 11169 (1996).

[68] G. Kresse and D. Joubert, Phys. Rev. B **59**, 1758 (1999).

[69] P. E. Blöchl, Phys. Rev. B **50**, 17953 (1994).

[70] J. P. Perdew, K. Burke, and M. Ernzerhof, Phys. Rev. Lett. **77**, 3865 (1996).